The 5th International Symposium - Supercritical CO_2 Power Cycles
March 28-31, 2016, San Antonio, Texas

THE EFFECT OF O_2 AND H_2O ON OXIDATION IN CO_2 AT 700°-800°C

Bruce A. Pint
Group Leader
Oak Ridge National Laboratory
Oak Ridge, TN 37831-6156 USA
pintba@ornl.gov

Robert G. Brese
PhD student
University of Tennessee
Knoxville, TN 37996 USA
breserg@ornl.gov

James R. Keiser
Distinguished R&D Staff Member
Oak Ridge National Laboratory
Oak Ridge, TN 37831-6156 USA
keiserjr@ornl.gov

Bruce Pint is the Group Leader of the Corrosion Science & Technology Group in the Materials Science & Technology Division at ORNL. He received his Ph.D. from M.I.T. in Ceramic Science and Engineering in 1992 and has been at ORNL since 1994. Dr. Pint is the principal investigator for numerous R&D projects including corrosion issues in fossil energy, nuclear energy, fusion energy and combined heat and power systems. His research covers compatibility, lifetime predictions, environmental effects and coatings in all types of power generation. He is a Fellow of NACE International and ASM International.

Robert Brese is a Ph.D student in the Bredesen Center at the University of Tennessee studying Energy Science and Engineering. He earned his B.S. in Materials Science and Engineering from The Ohio State University in 2014. Robert joined the Corrosion Science & Technology group in 2015.

James Keiser is a Distinguished Research and Development Staff Member and has worked in ORNL's Corrosion Science & Technology Group since 1974 where he has studied the compatibility of materials with the environments of energy producing systems. Studies have addressed the performance of metallic and ceramic materials in environments containing gaseous, liquid and supercritical corrodents. Several of his current projects concern corrosion issues in biomass liquefaction and gasification. Dr. Keiser received his B.S. in Materials Science and Ph.D. in Metallurgical Engineering and is a Fellow of NACE International and ASM International.

ABSTRACT

Direct-fired or open supercritical CO_2 (sCO_2) cycles are expected to have high impurity levels that may greatly alter the compatibility of structural alloys in these environments. However, there are no available laboratory facilities to simulate these environments at operating conditions of ~750°C and >100 bar. As an initial assessment of the effects of O_2 and H_2O on oxidation in a CO_2 environment, 500 h experiments were conducted at 1 bar at 700°-800°C in dry air, high-purity CO_2, CO_2+0.15%O_2 and CO_2+10%H_2O. A range of Fe- and Ni-base alloys, which form protective Cr- and Al-rich surface oxides, were evaluated. Oxide formation on a conventional stainless steel, 347HFG was increased by the addition of H_2O at 700° and 800°C, but not at 750°C. Similarly, the Fe-rich oxide on Grade 91 steel was greatly increased at all temperatures with the addition of H_2O. However, for the higher alloyed Fe- and Ni-base alloys, modifications in the environment did not strongly affect their reaction rates.

INTRODUCTION

The proposed direct-fired or open supercritical CO_2 (sCO_2) cycle [Allam 2013, Wright 2013] has the potential to achieve economical, "clean" fossil energy power generation. The CO_2 from the combustion of natural gas or coal-derived synthesis gas would be incorporated into the supercritical cycle as well as H_2O and O_2 residuals from the combustion process. Some of the CO_2 at the bottom of the cycle could then be diverted for sequestration or enhanced oil recovery. This cycle creates a more complex environment than the more conventional indirect-fired or closed sCO_2 cycle. Without significant impurities (typically ppm levels of O_2, H_2O, etc.), most studies have shown relatively good compatibility of highly alloyed Fe- and Ni-base structural alloys either at supercritical pressures [Oh 2006, Dunlevy, 2009, Gibbs, 2010, Rouillard 2011, Tan 2011, Moore 2012, Cao 2012, Firouzdor 2013, He 2014, Mahaffey 2014, Pint 2014a, Olivares 2015, Pint 2015a, Pint 2016a] or at ~40 bar for the UK gas cooled reactor program [Evans 1976, Garrett 1982]. Fast reaction rates were mainly observed on 9-12%Cr steels and conventional stainless steels. However, there are no current experimental facilities to simulate the open cycle impurities of 1-10%H_2O and 1-3%O_2 under supercritical pressures. In 1 bar testing, the addition of H_2O to CO_2 has been found to result in much faster oxidation rates, especially for Fe-base alloys [Kranzmann 2009, Quadakkers 2011, Gheno 2012, Gheno 2013, Nguyen 2014, Pint 2014b]. At high pressure, these levels of H_2O and O_2 could react with Cr-rich reaction products to form volatile Cr oxy-hydroxides [Young 2006, Holcomb 2009], which can significantly accelerate the degradation of highly-alloyed Fe- and Ni-base alloys [Pint 2011, Pint 2012, Bender 2014]. The current study is an initial assessment of the effect of H_2O and O_2 additions in 1 bar CO_2 at 700°-800°C on the oxidation behavior of representative structural alloys for sCO_2 systems. This temperature range is of interest to achieve ≥50% efficiency [Feher 1968]. The structural materials of interest include solid solution and precipitation-strengthened Ni-base alloys identified by the U.S. Advanced Ultrasupercritical Steam Consortium [Viswanathan 2005, Viswanathan 2010]; alumina-forming alloys which have been found to be less permeable to C in carburizing environments [e.g. Jönsson 1997] and more stable in the presence of H_2O [e.g. Pint 2011]; and lower cost Fe-base alloys including model alloys to identify the critical Cr content to resist accelerated attack in these environments. After these 500h exposures, only the lower alloyed Fe-base alloys showed rapid attack, especially in the CO_2-H_2O environment.

EXPERIMENTAL PROCEDURE

The exposures were conducted at 1 bar in a horizontal alumina tube with end caps within a 3-zone furnace. Table 1 lists the measured compositions of the alloys exposed in this study. Alloy specimens were typically ~1.5 x 11 x 19 mm with a final 600 grit surface finish on all sides. The coupons were ultrasonically cleaned in acetone and methanol prior to exposure and held in a pre-annealed alumina boat. The specimens were slowly heated to temperature in argon over several hours (~2°C/min), held for 500 h at temperature ±2°C in the oxidizing gas and then cooled in argon to room temperature inside the furnace. Experiments were conducted at 700°, 750° and 800°C in dry air, high-purity CO_2 (specifications of <5 ppm moisture and <5 ppm total hydrocarbons), CO_2 with 0.15%O_2 and CO_2+10vol.%H_2O with the H_2O atomized into the CO_2 carrier gas. Mass change was measured on a Mettler Toledo model XP205 balance (±0.04 mg accuracy or ±0.01 mg/cm^2). After exposure, specimens were Cu-plated to protect the surface oxide and metallographically mounted and imaged with light microscopy.

Table 1. Chemical composition of the alloys measured by inductively coupled plasma and combustion analyses in mass%. UNS numbers are included where available.

Alloy	Fe	Ni	Cr	Al	Other
Ferritic chromia-forming steels					
Gr.91 (S90901)	89.7	0.1	8.3	<	1Mo,0.3Mn,0.1Si, 0.08C
FeCrMo (S44735)	72.6	0.1	25.8	<	1.0Mo,0.2Si,0.1V
Fe-12.5Cr	86.7	<	12.4	0.01	0.6Mn,0.2Si,0.005Y
Fe-15Cr	84.1	<	14.9	0.02	0.6Mn,0.3Si,0.012Y
Fe-17.5Cr	81.6	<	17.5	0.02	0.6Mn,0.3Si,0.011Y
Fe-20Cr	79.0	<	20.0	0.02	0.7Mn,0.3Si,0.010Y
Fe-22.5Cr	76.6	<	22.5	0.01	0.2Mn,0.7Si,0.002Y
Fe-25Cr	74.0	<	25.0	0.01	0.7Mn,0.3Si,0.002Y
Austenitic Fe-base chromia-forming steels					
347HFG (S34710)	66.0	11.8	18.6	0.01	1.5Mn,0.8Nb,0.4Si,0.2Mo,0.2Co,0.09C
310HCbN (S31042)	51.3	20.3	25.5	<	0.3Co,0.4Nb,1.2Mn,0.3Si,0.3N,0.05C
Fe-base alumina-forming alloys					
FeCrAlMo	69.2	0.2	21.1	5.0	0.2Hf,0.1Mn,2.8Mo,0.6Si,0.3Y,0.1Zr
AFA OC4	49.1	25.2	13.9	3.5	2.5Nb,2W,1.9Mn,2Mo,0.5Cu,0.2Si,0.1C
CAFA	48.4	25.2	14.6	3.5	1.0Nb,1.3W,2Mn,1.9Mo,0.6Cu,0.9Si,0.4C
DAFA	44.5	33.3	14.0	2.7	2.8Nb,1.7Ti,0.2Mn,0.4Si,0.1C
Ni-base chromia-forming alloys					
625 (N06625)	4.0	60.6	21.7	0.09	9.4Mo,3.6Nb,0.2Ti,0.2Si,0.1Mn
230 (N06230)	1.5	60.5	22.6	0.3	12.3W,1.4Mo,0.5Mn,0.4Si
CCA617 (N06617)	0.6	55.9	21.6	1.3	11.3Co,8.6Mo,0.4Ti,0.1Si
282 (N07208)	0.2	58.0	19.3	1.5	10.3Co,8.3Mo,0.06Si,2.2Ti,0.1Mn
740 (N07740)	1.9	48.2	23.4	0.8	20.2Co,2.1Nb,2.0Ti,0.3Mn,0.5Si
Ni-base alumina-forming alloys					
214 (N07214)	3.5	75.9	15.6	4.3	0.2Mn,0.1Si,0.02Zr
247 (N07247)	0.07	59.5	8.5	5.7	9.8Co,9.9W,0.7Mo,3.1Ta,1.0Ti,1.4Hf

< indicates less than 0.01%

RESULTS

Figures 1-3 summarize the mass change data at each temperature. At 700°C, most of the specimens exhibited low mass gains consistent with a thin protective scale, Figure 1. The exceptions were the Gr.91 specimens, which could not form a protective scale in air at this temperature. However, the mass gain was an order of magnitude higher for the Gr.91 specimen exposed in the CO_2-H_2O environment. This environment also caused severe attack of the 347HFG specimen, which is consistent with other studies of similar "wet" CO_2 environments [Quadakkers 2011, Gheno 2012, Gheno 2013, Nguyen 2014]. The higher-alloyed specimens did not appear to be significantly affected by the addition of H_2O at 700°C.

Similar results were observed at 750°C, Figure 2. However, the 347HFG specimen was able to form a protective scale in all four environments. At 800°C, a protective scale formed on the Gr.91 specimens in air and CO_2, Figure 3. Again, the CO_2-H_2O environment severely attacked the Gr.91 specimen. The 347HFG specimens exposed in CO_2 and CO_2-H_2O showed a mass loss at this temperature and the E-Brite specimen showed no mass change in the CO_2-H_2O environment. Alloy 625 showed an unexpected large mass gain in CO_2 but not in CO_2-H_2O. The CO_2-O_2

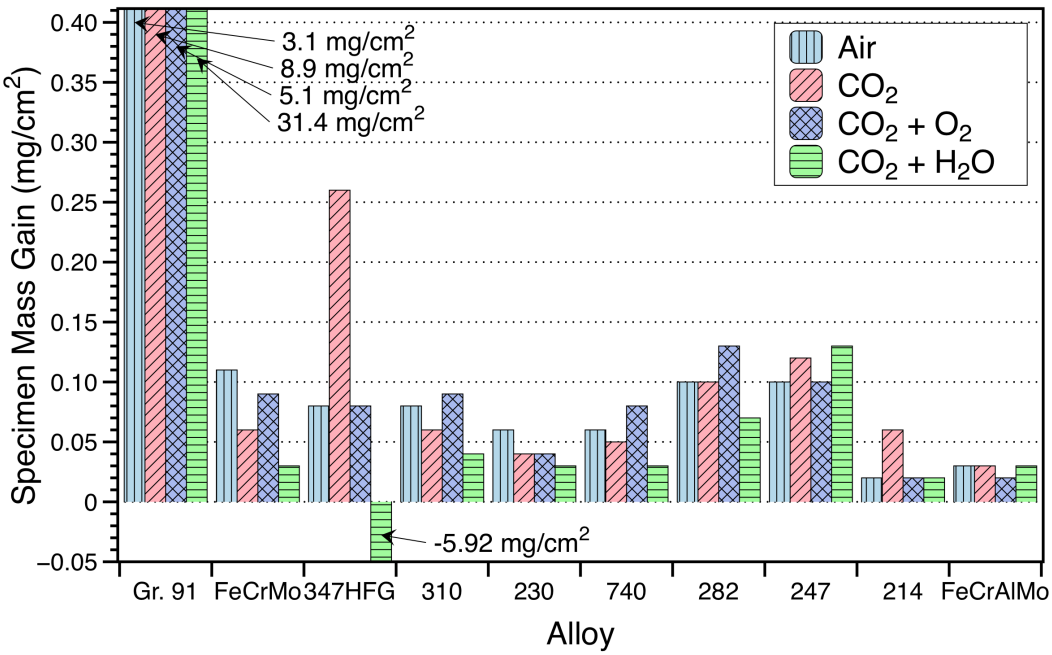

Figure 1. Specimen mass gain data for 500 h exposures in 1 bar experiments at 700°C. Data from Pint 2014a.

experiment at 800°C was not conducted.

Figures 4-6 show light microscopy of polished cross-sections of representative specimens at each temperature. Both high and low magnification images of the Gr.91 specimens exposed at 700°C

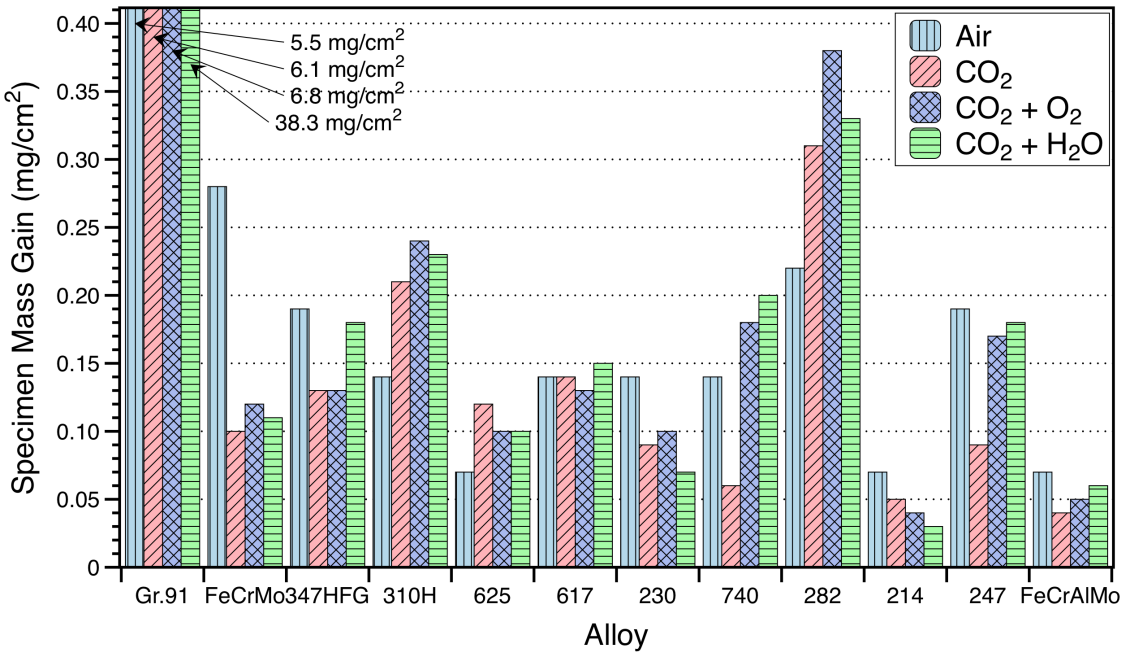

Figure 2. Specimen mass gain data for 500 h exposures in 1 bar experiments at 750°C.

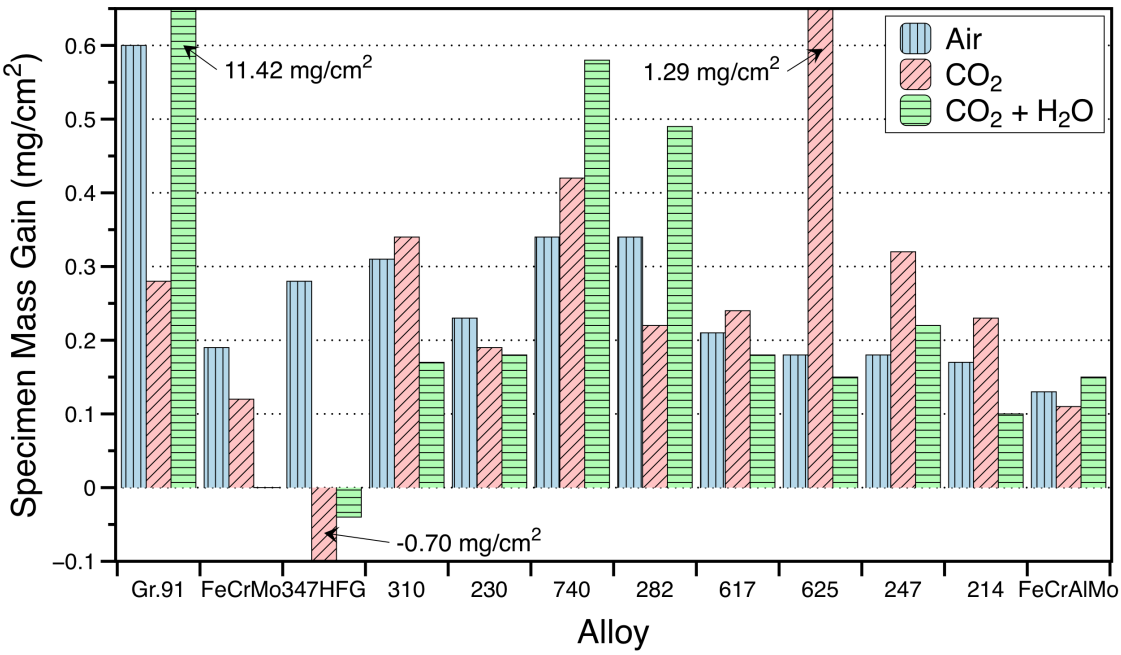

Figure 3. Specimen mass gain data for 500 h exposures in 1 bar experiments at 800°C.

are shown in Figure 4 because the scale was not uniform in all cases. In dry air, the scale on the Gr.91 specimen appeared uniform across the entire specimen with the typical duplex scale structure observed on low-alloyed steels [e.g. Gheno 2012, Pint 2014a, Nguyen 2015]. In CO_2, the scale was non-uniform with some areas forming a thin protective scale, while a very thick oxide formed on some areas. A similar combination of protective and non-protective oxide was observed in O_2-buffered CO_2. In this case, the non-protective oxide was not as thick as was observed in high purity CO_2 and similar to the scale formed in dry air. In CO_2-H_2O, the scale again appeared fairly uniform with variations likely due to scale spallation of the 200+µm thick oxide. The duplex oxide typically consists of an inner spinel-type Fe-Cr oxide and an outer FeO_x layer. In this case, the outer layer consisted of an light gray layer of Fe_2O_3 at the gas interface with an underlying Fe_3O_4 layer. For the 347HFG specimens, only minor oxide nodules were observed in CO_2. However, a much thicker scale was observed after exposure in CO_2-H_2O. In this case, typical of austenitic steels with a higher thermal expansion, the outer FeO_x layer has spalled resulting in a large mass loss (Figure 1) and only the inner spinel-type oxide remained. For the higher-alloyed specimens shown in Figure 4, 310HCbN, 230, 282 and 214, the scales were mainly uniform, thin and protective. For the very thin flat oxides, adhesion of the Cu plating was an issue in some cases and what appears to be a thicker reaction product is only a gap between the plating and the reaction product, e.g. 310HCbN in CO_2-O_2 and CO_2-H_2O. The slightly higher mass gains for the 282 specimens may be attributed to the Al and Ti additions in this alloy. These elements can internally oxidize and Ti is known to accelerate the growth of Cr_2O_3 [Ennis 1985, Brady 2006, Pint 2014c]. A thin Al-rich oxide formed on alloy 214 in all cases at 700°C, consistent with the low mass gains, Figure 1.

Figure 5 shows similar structures after exposures at 750°C. The lower magnification images of Gr.91 show non-uniform attack, except perhaps for the CO_2-H_2O environment where a thick oxide

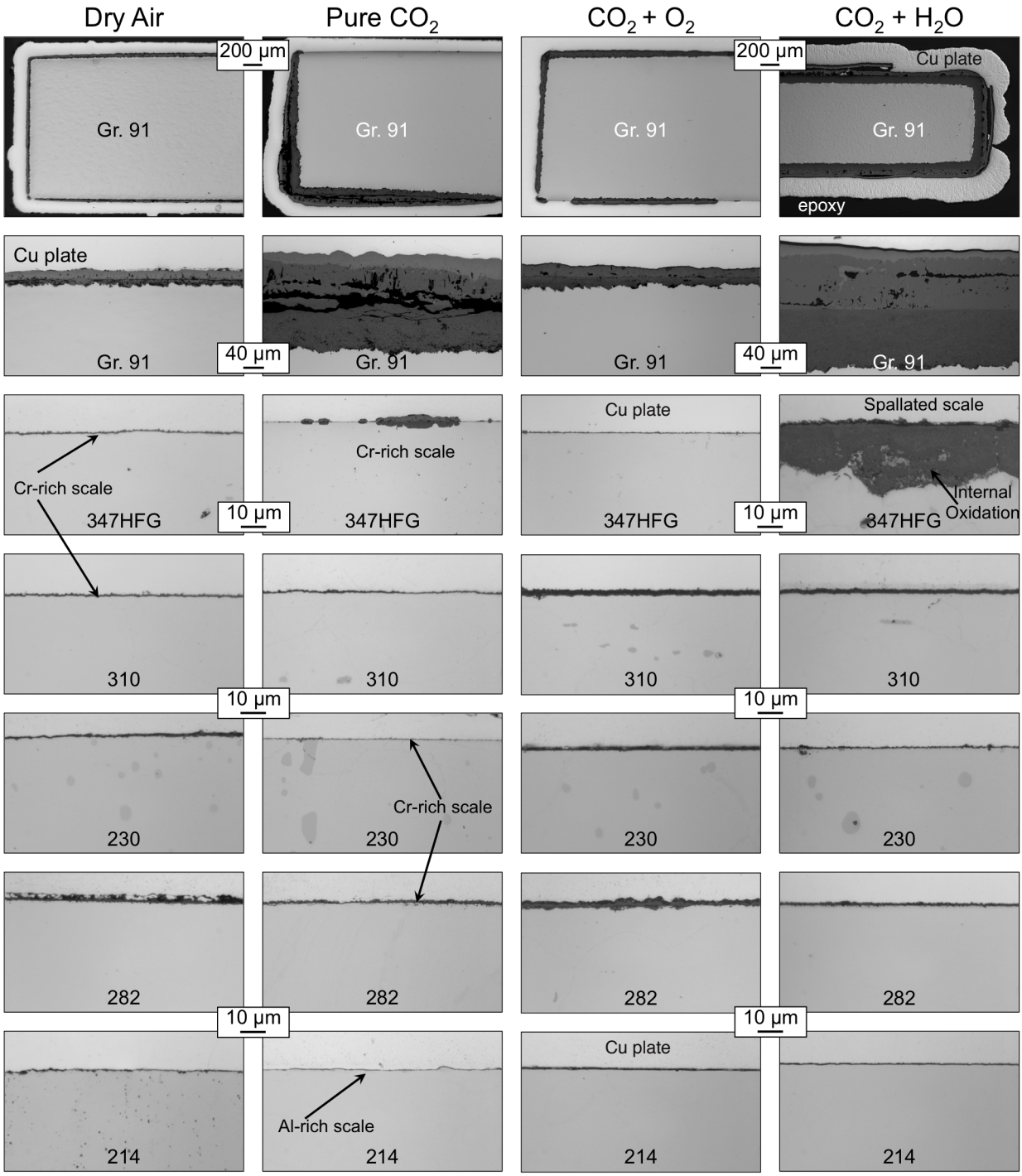

Figure 4: Light microscopy of polished cross-sections of specimens exposed for 500 h at 700°C in four different environments.

formed across the entire specimen. A similar duplex structure also was observed at this temperature. After 500 h at this temperature, the 347HFG specimens did not experience accelerated oxidation. The other alloys shown, including FeCrMo and 625, formed similar thin

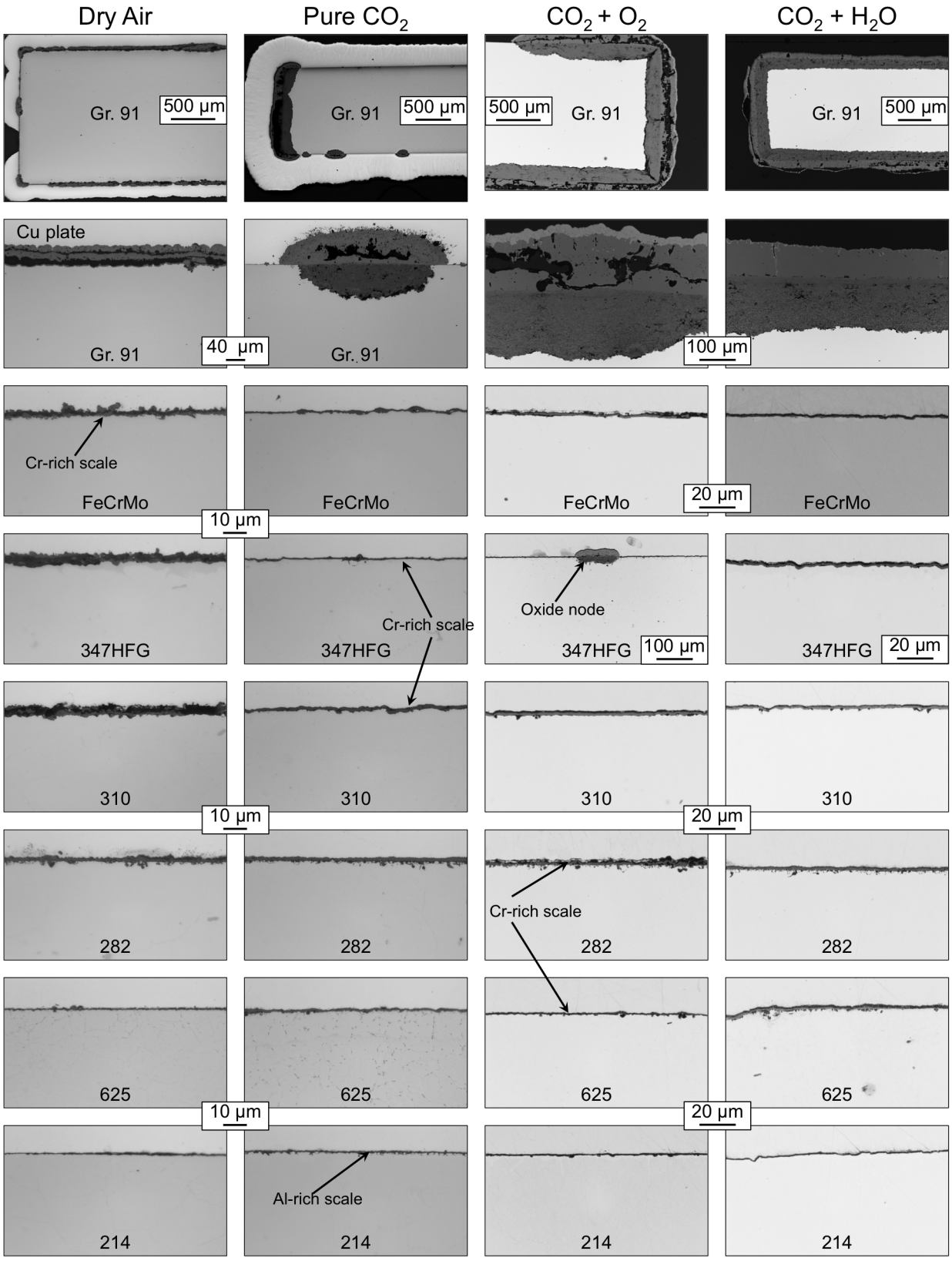

Figure 5. Light microscopy of polished cross-sections of specimens exposed for 500 h at 750°C in four different environments.

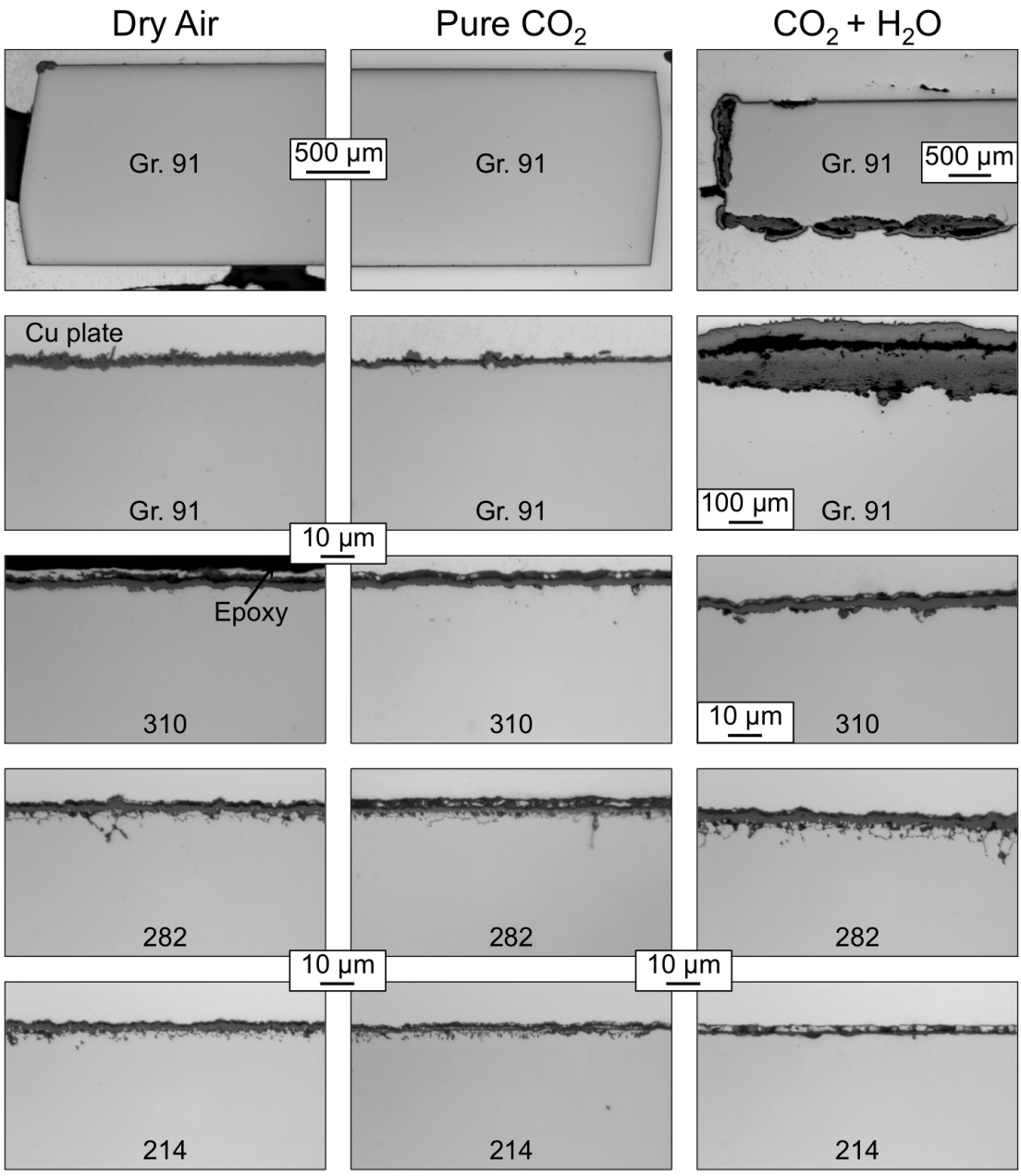

Figure 6. Light microscopy of polished cross-sections of specimens exposed for 500 h at 800°C in three different environments.

oxides in all four environments. At this temperature, the internal oxidation on the 282 specimens was more evident as this alloy contains much more Al and Ti than the other chromia-forming alloys, Table 1. Again, very thin oxides were observed on alloy 214, consistent with the very low mass gains shown in Figure 2.

Figure 6 shows examples of the specimens exposed at 800°C. The oxides formed on the Gr.91 specimens exposed in dry air and CO_2 were remarkably protective with low mass gains consistent with the thin oxides observed, Figure 3. As at lower temperatures, with the addition of H_2O, a much thicker reaction product formed with the typical duplex microstructure. In this case, the lower

magnification images show that the thick oxide was not uniform across the surface. For the other alloys shown in Figure 6, generally thicker reaction products were observed, which can be attributed to the higher exposure temperature. Once again, more distinct internal oxidation was observed for the alloy 282 specimens. Like the 740 specimen, the 282 specimen had a higher mass gain in the CO_2+H_2O environment, perhaps forming a thicker scale compared to CO_2, Figure 6. A previous study characterized the internal oxidation kinetics of 740 and 282 to 5,000–10,000 h in 1 bar dry air, air+10%H_2O and steam at 800°C and found low parabolic reaction rates [Pint 2015b]. Except for the 740 and 282 specimens, there was no significant indication of a negative effect of water vapor on the higher alloyed specimens. As expected, the thinnest reaction products were observed for the alumina-forming alloy 214 specimens, Figure 6.

At 800°C, several different alumina-forming alloys were exposed to compare to the baseline Ni-base alloys 214 and 247 and the ferritic FeCrAlMo alloy, Figure 7. The additional alloys are from a family of high creep strength, Fe-base alumina-forming austenitic (AFA) alloys [Brady 2008, Yamamoto 2011, Yamamoto 2013, Muralidharan 2015] including wrought and cast (CAFA) versions. The conventional wrought AFA alloy OC4 exhibited mass gains similar to the other alumina formers. However, the cast AFA specimens showed slightly higher mass gains. The highest strength, γ′-strengthened DAFA alloy specimens showed relatively low mass gains in dry air and CO_2 but a relatively high mass gain in CO_2+H_2O. This alloy also contained the lowest Al content, which may explain the results, Table 1. Figure 8 compares the reaction products on the AFA alloy specimens to that formed on the FeCrAlMo specimen after exposure in the CO_2-H_2O environment. Consistent with the mass change results, the scale on AFA OC4 was similar to that formed on FeCrAlMo. A thicker scale and internal oxidation was observed on the cast AFA specimen and the higher mass gain for the DAFA specimen was due to internal oxidation and some Fe-rich oxide nodule formation, Figure 8.

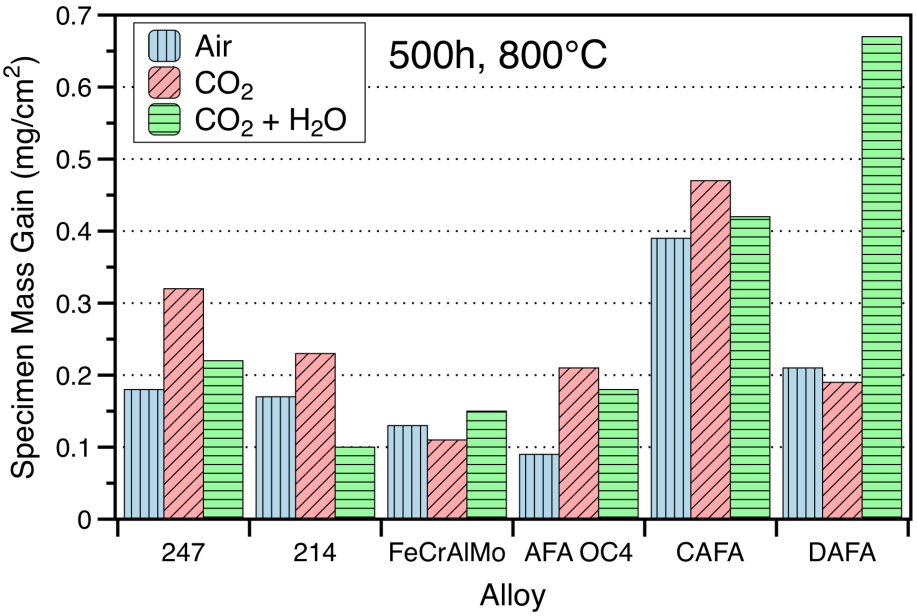

Figure 7. Specimen mass gain data for alumina-forming alloys in 500 h exposures in 1 bar experiments at 800°C.

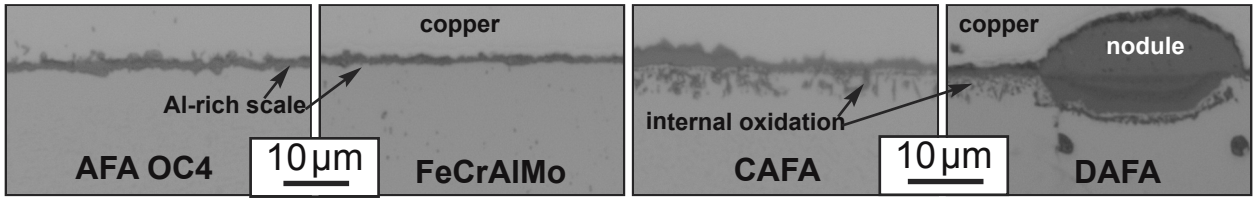

Figure 8. Light microscopy of polished cross-sections of alumina-forming alloy specimens exposed for 500 h at 800°C in CO_2+H_2O.

Finally, to gain more understanding about the role of Cr content in forming protective Cr-rich oxides in these environments, a series of model Fe-Cr+Mn,Si,Y alloys (Table 1) also were exposed at 800°C, Figure 9. In 1 bar CO_2, it appeared that the specimens with ≤17.5%Cr had a higher mass gain, suggesting a thicker oxide than the higher Cr specimens. This trend was repeated in CO_2-H_2O, so the addition of H_2O did not appear to affect the critical Cr content needed for protective behavior after 500 h. In dry air, the 12.5%Cr specimen exhibited an unusually high mass gain, while the other specimens showed no distinct differentiation in mass gain based on alloy Cr content, Figure 9. In contrast to the mass change data, Figure 10 shows the thin Cr-rich oxides formed on most of the surface in all three environments for both the 12.5%Cr and the 20%Cr specimens. In CO_2-H_2O, the higher mass gain for the 12.5%Cr specimen (compared to the 20%Cr specimen) was due to Fe-rich oxide nodule formation at the edges and corners of the specimen (not shown in Figure 10).

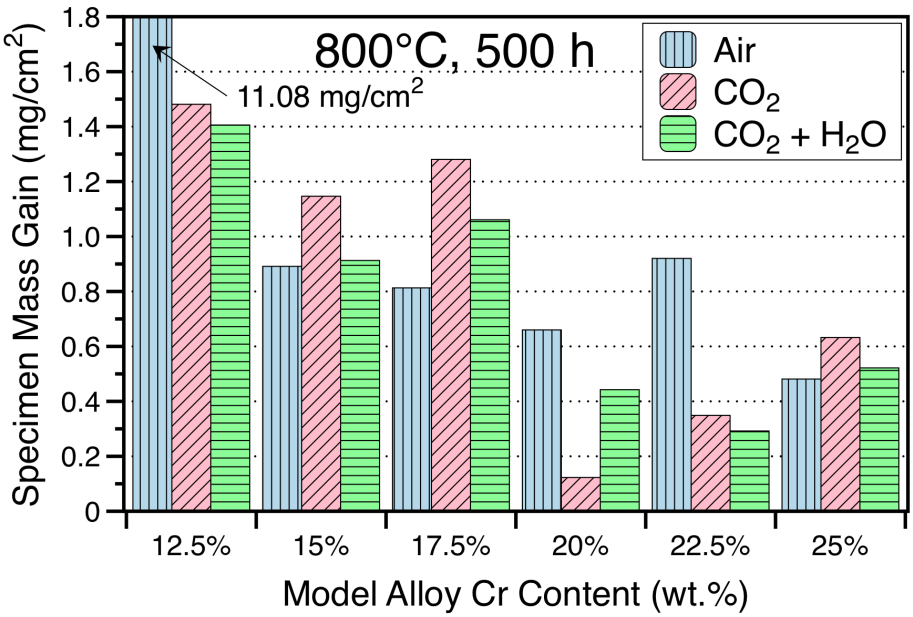

Figure 9. Specimen mass gain data for model Fe-Cr+Mn,Si,Y alloys in 500 h exposures in 1 bar experiments at 800°C.

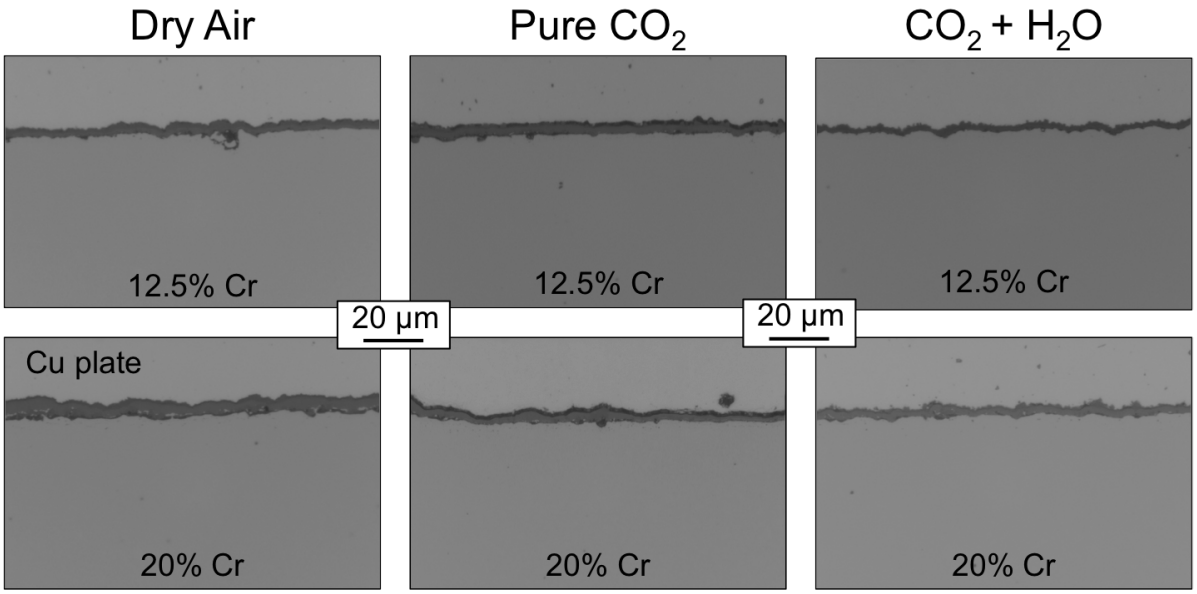

Figure 10. Light microscopy of polished cross-sections of model Fe-Cr alloy specimens exposed for 500 h at 800°C in three different environments.

DISCUSSION

These results are very preliminary with only 500 h exposures. While CO_2 pressure has only shown minor effects on reaction rates at 650°-750°C [Pint 2016b], the same may not be true for impurity effects. More work is needed to study impurity effects under supercritical conditions for direct-fired sCO_2 concepts. An autoclave system with on-line impurity monitoring is being constructed at ORNL for this purpose. As mentioned in the introduction, one possible effect of higher pressure is that the higher total pressures of O_2 and H_2O could react with the Cr-rich reaction products on structural alloys such as 740 and form volatile Cr oxy-hydroxides [Young 2006, Holcomb 2009], which would then accelerate the loss of Cr from the alloy substrate. This is a particular concern for thin-walled components in heat exchangers.

Consistent with previous 1 bar results [Quadakkers 2011, Gheno 2012, Gheno 2013, Nguyen 2014, Pint 2014b], the lower-alloyed Fe-base alloys (i.e. Gr.91 and 347HFG) appeared to be more susceptible to accelerated attack (i.e. the rapid formation of Fe-rich oxide nodules rather than a thin, protective Cr-rich oxide), especially with the addition of H_2O. The addition of O_2 did not have particularly detrimental effects under these conditions and was not investigated at 800°C. Oxygen could have a beneficial effect by facilitating the formation of a protective scale on the higher-alloyed materials. On the low alloy steels, it could have a negative effect by increasing the growth rate of Fe-rich oxides, as was observed for the Gr.91 specimens. (It should be noted again that the mass gain data for the Gr.91 specimens may be affected by scale spallation.) For low alloy steels, a similar study may be warranted at lower temperatures (e.g. 400°-600°C) where they are more likely to be structural candidates. Also, more work is needed to look for signs of internal carburization in these specimens as has been seen in other studies [e.g. Rouillard 2011, Quadakkers 2011, Gheno 2012, Gheno 2013, Nguyen 2014].

For sCO_2 applications above 700°C, Ni-base alloys are the most likely structural alloy candidates, especially the precipitation strengthened alloys 740 [Zhao 2003, Shingledecker 2013] and 282

[Pike 2008]. At these temperatures, these alloys have been found to be very oxidation resistant in a variety of environments up to 800°C [Pint 2015b]. The mass gains are slightly higher for these alloys, especially 282 at 750°C and 740 at 800°C, Figures 2 and 3. This is attributed to the internal oxidation of Al and Ti for these alloys, and possibly the Nb in 740. The high temperature oxidation resistance of these alloys at 1 bar is also relevant for the primary heat exchanger on indirect-fired systems, which will need to operate at higher temperatures to achieve a peak sCO_2 temperature above 700°C for >50% efficient designs [Feher 1968].

Several alumina-forming alloys were evaluated, especially at the highest temperatures, because of the potentially lower reaction rates and higher thermodynamic stability of Al_2O_3. Alumina scales are thought to be less permeable to carbon (or carbonaceous species) [e.g. Jönsson 1997]. Also, alumina-forming alloys have been shown to very protective even in the presence of H_2O and O_2. Whereas chromia-forming alloys can form volatile $CrO_2(OH)_2$ in such mixed oxidation environments [Asteman 1999, Young 2006, Holcomb 2009], alumina is relatively unaffected [Brady 2008, Yamamoto 2011, Pint 2011, Yamamoto 2013, Muralidharan 2015]. A concern for sCO_2 systems is that alumina can be difficult to form at <700°C because of slow diffusion of Al in the alloy and relatively low Al contents in these structural alloys, Table 1. In fact, prior work at 650°C and 200 bar sCO_2 showed imperfect alumina formation after 500 h on several alumina-forming alloys including 214 and AFA OC4 [Pint 2014a]. The performance of superalloy 247 was additionally complicated by the presence of Hf-rich carbides. Characterization of the oxidation of these carbides in sCO_2 environments was reported elsewhere [Pint 2015a].

The model alloys were evaluated to see if H_2O affected the critical Cr content needed to form a protective scale at 800°C, Figure 9. However, all of the alloys formed protective oxides over the majority of their surface during these 500 h exposures, Figure 10. This may be due to the relatively short exposure or the beneficial effects of the Mn, Si and Y additions to these alloys, Table 1. During short exposures, scales can remain protective during an incubation period followed by accelerated oxidation (i.e. Fe-rich oxide formation) when the scale breaks down or the adjacent alloy becomes Cr depleted. Comparing the 12.5%Cr model alloy results to those for Grade 91 (with only 8.3%Cr, Table 1), the mass gains for the 12.5%Cr specimens in air and CO_2 were actually higher than for the Grade 91 specimens. However, the 12.5%Cr specimen showed a much lower mass gain than the Grade 91 specimen in CO_2-H_2O, Figure 3. The more protective behavior could be due to the higher Cr content. Both alloys have additions of Mn and Si, which are potentially protective elements that form oxide layers: Mn typically at the gas interface and Si at the metal-scale interface [Nguyen 2015]. Longer exposures might show that both alloys form thick, duplex scales after an incubation period.

The characterization shown to date is somewhat limited as this work is still in progress. However, additional long-term testing is also needed to verify these short-term results. Most likely these long-term experiments will be conducted at both high pressure and 1 bar because of the limited experimental facilities available. The results of additional laboratory testing may assist in risk reduction for the building of a direct-fired sCO_2 pilot plant.

CONCLUSIONS

In order to study the effect of O_2 and H_2O impurities on a direct-fired sCO_2 system, initial work was conducted with 500 h exposures at 1 bar including comparison experiments in dry air to establish a baseline for reaction rates at 700°-800°C. A broad range of representative Fe- and

Ni-base alloys was exposed in order to provide information on performance under these conditions. For the relatively low alloyed steels like Gr.91 (Fe-9Cr-1Mo) and 347HFG, the addition of H_2O tended to accelerate the rate of attack at these temperatures due to the formation of nodules or thick Fe-rich duplex oxides. However, because the reaction kinetics are related to both transport in the reaction product and in the underlying alloy substrate, the effect of temperature can be complicated with higher temperatures resulting in more protective behavior because of faster Cr transport in the metal. For the higher alloyed Fe-base and Ni-base alloys, very little effect of environment was observed at all three temperatures. In this temperature range, most alumina-forming alloys formed thin, protective scales and may be candidates for certain applications because of their superior oxidation resistance and oxide stability. Clearly, longer-term experiments and experiments with impurities at high pressure are needed to further study this compatibility issue.

NOMENCLATURE

AFA = alumina-forming austenitic (steel)
APMT = Advanced Powder Metallurgy Tube (Sandvik/Kanthal FeCrAl alloy)
Gr. = Grade (steel)
HFG = H (high carbon) FG (fine grain structure)
ORNL = Oak Ridge National Laboratory
UK = United Kingdom

REFERENCES

Allam, R. J., Palmer, M. R., Brown Jr., G. W., Fetvedt, J., Freed, D., Nomoto, H., Itoh, M., Okita, N., Jones Jr., C., 2013a, “High efficiency and low cost of electricity generation from fossil fuels while eliminating atmospheric emissions, including carbon dioxide,” Energy Procedia 37, 1135–1149.

Asteman, H., Svensson, J.-E., Johansson, L.-G., Norell, M., 1999, “Indication of Chromium Oxide Hydroxide Evaporation During Oxidation of 304L at 873K in the Presence of 10% Water Vapor,” Oxid. Met. 52, 95-111.

Bender, M. D., Klug, R. C., 2014, “Comparison of Ni-Based 625 Alloy and ATI 20-25+Nb™ Stainless Steel Foils After Long-Term Exposure to Gas Turbine Engine Exhaust,” ASME Paper #GT2014-25334, presented at the International Gas Turbine & Aeroengine Congress & Exhibition, Düsseldorf, Germany, June 16–20, 2014.

Brady, M. P., Pint, B. A., Lu, Z. G., Zhu, J. H., Milliken, C. E., Kreidler, E. D.. Miller, L., Armstrong, T. R., Walker, L. R., 2006, “Comparison of Oxidation Behavior and Electrical Properties of Doped NiO- and Cr2O3-Forming Alloys for Solid Oxide Fuel Cell Metallic Interconnects,” Oxid. Met. 65, 237-261.

Brady, M. P., Yamamoto, Y., Santella, M. L., Maziasz, P. J., Pint, B. A., Liu, C. T., Lu, Z. P., Bei, H., 2008,“The Development of Alumina-Forming Austenitic Stainless Steels for High-Temperature Structural Use,” JOM 60(7), 12-18.

Cao, G., Firouzdor, V., Sridharan, K., Anderson, M., Allen, T. R., 2012, “Corrosion of austenitic alloys in high temperature supercritical carbon dioxide,” Corros. Sci. 60, 246-255.

Dunlevy, M. W., 2009, “An Exploration of the Effect of Temperature on Different Alloys in

Supercritical Carbon Dioxide Environment," M.Sc. Thesis, MIT, Cambridge, MA.

Ennis P. J., Quadakkers, W. J., 1985, "Corrosion and Creep of Nickel-Base Alloys in Steam Reforming Gas," in High Temperature Alloys, Their Exploitable Potential, eds. J. B. Marriott, M. Merz, J. Nihoul and J. Ward, Elsevier, London, p.465-74.

Evans, H. E., Hilton, D. A. and Holm, R. A., 1976, "Chromium-Depleted Zones and the Oxidation Process in Stainless Steels," Oxid. Met. 10, 149-161.

Feher, E. G., 1968, "The Supercritical Thermodynamic Power Cycle," Energy Conversion, 8, 85-90.

Firouzdor, V. Sridharan, K., Cao, G., Anderson, M. Allen, T. R., 2013, "Corrosion of a stainless steel and nickel-based alloys in high temperature supercritical carbon dioxide environment," Corrosion Science 69, 281-291.

Garrett, J. C. P., Crook, J. T., Lister, S. K., Nolan, P. J., Twelves, J. A., 1982, "Factors in the Oxidation Assessment of AISI Type 310 Steels in High Pressure Carbon Dioxide," Corros. Sci. 22, 37-50.

Gheno, T., Monceau, D., Young, D. J., 2012, "Mechanism of breakaway oxidation of Fe-Cr and Fe-Cr-Ni alloys in dry and wet carbon dioxide," Corros. Sci., 64, 222-233.

Gheno, T., Monceau, D., Young, D. J., 2013, "Kinetics of breakaway oxidation of Fe-Cr and Fe-Cr-Ni alloys in dry and wet carbon dioxide," Corros. Sci. 77, 246-256.

Gibbs, J. P., 2010, "Corrosion of Various Engineering Alloys in Supercritical Carbon Dioxide Environment," M.Sc. Thesis, MIT, Cambridge, MA.

He, L. F., Roman, P., Leng, B., Sridharan, K., Anderson, M. Allen, T. R., 2014, "Corrosion behavior of an alumina forming austenitic steel exposed to supercritical carbon dioxide," Corrosion Science 82, 67–76.

Holcomb, G. R., 2009, "Steam Oxidation and Chromia Evaporation in Ultrasupercritical Steam Boilers and Turbines," J. Electrochem. Soc. 156 (9), C292-C297.

Jönsson, B., Svedberg, C., 1997, "Limiting Factors for Fe-Cr-Al and NiCr in Controlled Industrial Atmospheres," Mater. Sci. Forum, 251-254 (1997) 551-558.

Kranzmann, A., Huenert, D., Rooch, H., Urban, I., Schulz, W., Oesterle, W., 2009, "Reactions at the interface between steel and oxide scale in wet CO_2 containing atmospheres," NACE Paper 09-265, Houston, TX, presented at NACE Corrosion 2009, Atlanta, GA, March 2009.

Mahaffey, J., Kaira, A., Anderson, M., Sridharan, K., 2014 "Materials Corrosion in High Temperature Supercritical Carbon Dioxide," in Proceedings of the 4th International Symposium on Supercritical CO_2 Power Cycles, Pittsburgh, PA, Paper #2.

Moore, R., Conboy, T., 2012, "Metal Corrosion in a Supercritical Carbon Dioxide – Liquid Sodium Power Cycle," Sandia National Laboratory Report SAND2012-0184.

Muralidharan, G., Yamamoto, Y., Brady, M. P., Pint, B. A., Voke, D., Pankiw, R. I., 2015, "Development of Cast Alumina-forming Austenitic Stainless Steel Alloys for use in High Temperature Process Environments," NACE Paper C2015-6114, Houston, TX, presented at NACE Corrosion 2015, Dallas, TX, March 2015.

Nguyen, T. D., Zhang, J. Q., Young, D. J., 2014, “Water vapour effects on corrosion of Fe-Cr and Fe-Cr-Ni alloys containing cerium and manganese in CO_2 gas at 818°C,” Corros. Sci. 89, 220-235.

Nguyen, T. D., Zhang, J. Q., Young, D. J., 2015, “Microstructures of chromia scales grown in CO_2,” Mater. High Temp. 32, 16-21.

Oh, C. H., Lillo, T., Windes, W., Totemeier, T., Ward, B., Moore, R., Barner, R., 2006, “Development Of A Supercritical Carbon Dioxide Brayton Cycle: Improving VHTR Efficiency And Testing Material Compatibility,” Idaho National Laboratory Report INL/EXT-06-01271.

Olivares, R. I., Young, D. J., Marvig, P., Stein, W., 2015, “Alloys SS316 and Hastelloy-C276 in Supercritical CO_2 at High Temperature,” Oxid. Met. 84, 585–606.

Pike, L. M., 2008, “Development of a Fabricable Gamma-Prime (γ’) Strengthened Superalloy,” in *Superalloys 2008*, R. C. Reed et al. eds TMS, Warrendale, PA, 2008, p.191-200.

Pint, B. A., Brady, M. P., Yamamoto, Y., Santella, M. L., Maziasz, P. J., Matthews, W. J., 2011, “Evaluation of Alumina-Forming Austenitic Foil for Advanced Recuperators,” J. Eng. Gas Turb. Power, 133 (10), 102302.

Pint, B. A., Dryepondt, S., Rouaix-Vande Put, A., Zhang, Y., 2012, “Mechanistic-Based Lifetime Predictions for High Temperature Alloys and Coatings,” JOM, 64, 1454-1460.

Pint, B. A., Keiser, J. R., 2014a, “The Effect of Temperature on the sCO_2 Compatibility of Conventional Structural Alloys,” in Proceedings of the 4th International Symposium on Supercritical CO_2 Power Cycles, Pittsburgh, PA, September 2014, Paper #61.

Pint, B. A., Thomson, J. K., 2014b, “Effect of oxy-firing on corrosion rates at 600°-650°C,” Materials and Corrosion 65, 132-140.

Pint, B. A., 2014c, “The Use of Model Alloys to Study the Effect of Alloy Composition on Steam and Fireside Corrosion,” NACE Paper 14-4279, Houston, TX, presented at NACE Corrosion 2014, San Antonio, TX.

Pint B. A., Keiser, J. R., 2015a, “Initial Assessment of Ni-Base Alloy Performance in 0.1 MPa and Supercritical CO_2,” JOM 67(11), 2615-2620.

Pint, B. A.,Thiesing, B. P., 2015b, “Effect of Environment on the Oxidation Behavior of Commercial and Model Ni-Base Alloys,” NACE Paper C2015-5919, Houston, TX, presented at NACE Corrosion 2015, Dallas, TX.

Pint B. A., Brese, R. G., Keiser, J. R., 2016a, “Supercritical CO_2 Compatibility of Structural Alloys at 400°-750°C,” NACE Paper C2016-7747, Houston, TX, presented at NACE Corrosion 2016, Vancouver, Canada, March 2016.

Pint B. A., Brese, R. G., Keiser, J. R., 2016b, “Effect of Pressure on Supercritical CO_2 Compatibility of Structural Alloys at 750°C,” Materials and Corrosion, in press.

Quadakkers, W. J., Olszewski, T., Piron-Abellan, J., Shemet, V., Singheiser, L., 2011, “Oxidation of Metallic Materials in Simulated CO_2/H_2O-rich Service Environments Relevant to an Oxyfuel Plant,” Mater. Sci. Forum 696, 194-199.

Rouillard, F., Charton, F., Moine, G., 2011 “Corrosion Behavior of Different Metallic Materials in Supercritical Carbon Dioxide at 550°C and 250 bars,” Corrosion 67(9), 095001

Shingledecker, J. P., Pharr, G. M., 2013, “Testing and Analysis of Full-Scale Creep-Rupture Experiments on Inconel Alloy 740 Cold-Formed Tubing,” J. Mater. Eng. Performance, 22, 454-462.

Tan, L. Anderson, M., Taylor, D., Allen, T. R., 2011, “Corrosion of austenitic and ferritic-martensitic steels exposed to supercritical carbon dioxide,” Corrosion Science 53, 3273-3280.

Viswanathan, R., Henry, J.F., Tanzosh, J., Stanko, G., Shingledecker, J., Vitalis, B., Purgert, R., 2005, “U.S. Program on Materials Technology for Ultra-Supercritical Coal Power Plants,” J. Mater. Eng. Performance 14(3), 281-285.

Viswanathan, R., Shingledecker, J., Purgert, R., 2010, “Evaluating Materials Technology for Advanced Ultrasupercritical Coal-Fired Plants,” Power, 154(8), 41-45.

Wright, I. G., Pint, B. A., Shingledecker, J. P., Thimsen, D., 2013, “Materials Considerations for Supercritical CO_2 Turbine Cycles,” ASME Paper #GT2013-94941, presented at the International Gas Turbine & Aeroengine Congress & Exhibition, San Antonio, TX, June, 3-7, 2013.

Yamamoto, Y., Brady, M. P., Santella, M. L., Bei, H., Maziasz, P. J., Pint, B. A., 2011, “Alloy Design Concept for High-Temperature Creep Resistance of Alumina-Forming Austenitic Stainless Steels,” Metallurgical and Materials Transactions A, 42 (2011) 922-931.

Yamamoto, Y., Muralidharan, G., Brady, M. P., 2013, “Development of $L1_2$-ordered $Ni_3(Al,Ti)$-strengthened alumina-forming austenitic stainless steel alloys,” Scripta Mater. 69, 816–819.

Young, D. J., Zhang, J., Geers C., Schütze, M., 2011, “Recent advances in understanding metal dusting: A review,” Materials and Corrosion 62, 7-28.

Zhao, S. Q., Xie, X. S., Smith, G. D. Patel, S. J., 2003, “Microstructural stability and mechanical properties of a new nickel based superalloy,” Mater. Sci. Eng. A 355, 96-105.

ACKNOWLEDGEMENTS

The experimental work at ORNL was conducted by M. Stephens, T. Lowe and T. Jordan. Material was provided by Haynes International, Special Metals, Allegheny-Ludlum, Sumitomo Metals, Capstone Turbines and Sandvik (Kanthal). P. F. Tortorelli and M. J. Lance provided useful comments on the manuscript. Research sponsored by the U. S. Department of Energy, Office of Fossil Energy, Coal and Power R&D. This manuscript has been authored by UT-Battelle, LLC under Contract No. DE-AC05-00OR22725 with the U.S. Department of Energy. The United States Government retains and the publisher, by accepting the article for publication, acknowledges that the United States Government retains a non-exclusive, paid-up, irrevocable, world-wide license to publish or reproduce the published form of this manuscript, or allow others to do so, for United States Government purposes. The Department of Energy will provide public access to these results of federally sponsored research in accordance with the DOE Public Access Plan (http://energy.gov/downloads/doe-public-access-plan).